Synthetic and Systems Biotechnology 10 (2025) 484–494

Contents lists available at ScienceDirect

Synthetic and Systems Biotechnology

journal homepage: www.keaipublishing.com/en/journals/synthetic-and-systems-biotechnology

Original Research Article

CRISPR-Cas9-based one-step multiplexed genome editing through optimizing guide RNA processing strategies in *Pichia pastoris*

Kaidi Chen [a,b,1], Gulikezi Maimaitirexiati [a,1], Qiannan Zhang [a], Yi Li [a,b], Xiangjian Liu [a], Hongting Tang [d], Xiang Gao [c], Bo Wang [c,***], Tao Yu [a,**], Shuyuan Guo [a,*]

[a] Center for Synthetic Biochemistry, CAS Key Laboratory of Quantitative Engineering Biology, Shenzhen Institute of Synthetic Biology, Shenzhen Institutes of Advanced Technology, Chinese Academy of Sciences (CAS), Shenzhen, 518055, China
[b] University of the Chinese Academy of Sciences, Beijing, 100049, China
[c] Center for Materials Synthetic Biology, CAS Key Laboratory of Quantitative Engineering Biology of CAS, Shenzhen Institute of Synthetic Biology, Shenzhen Institutes of Advanced Technology, Chinese Academic of Science, Shenzhen, 518055, China
[d] School of Agriculture and Biotechnology, Shenzhen Campus of Sun Yat-sen University, Sun Yat-sen University, Shenzhen, 518107, China

ARTICLE INFO

Keywords:
Pichia pastoris
Gene deletion and integration
CRISPR/Cas9
Genome editing
gRNA processing

ABSTRACT

The important methylotrophic yeast *Pichia pastoris* has been utilized for the production of a variety of heterologous recombinant proteins and has great potential for use in the production of value-added compounds using methanol as a substrate. However, the lack of convenient and efficient genome engineering tools has hindered further applications of *P. pastoris*, especially in complex and multistep metabolic engineering scenarios. Hence, we developed a rapid and convenient multi-gene editing system based on CRISPR/Cas9 by optimizing the guide RNA processing strategy, which can achieve dual-gene knockout or multi-gene integration in single step. Firstly, we found that the HgH (HH-sgRNA-HDV) structure achieved the highest single-gene knockout efficiency (95.8 %) among the three sgRNA processing cassettes, including a tRNA-sgRNA-tRNA (tgt) array, HgH structure and tRNA-sgRNA-HDV (tgH) structure. Furthermore, the dHgH structure (double HgH) enabled one-step dual-gene disruption and multi-gene integration. The efficiency of dual-site knockout ranged from 60 % to 100 %, with functional genes knockout achieving approximately 60 % (*Δaox1Δgut1*), while dual neutral sites knockout reached 100 %. Finally, we applied the system for one-step production of fatty acids and 5-hydroxytryptophan. The yield of FFAs reached 23 mg/L/μg protein/OD, while the yield of 5-hydroxytryptophan was 13.3 mg/L. The system will contribute to the application of *P. pastoris* as an attractive cell factory for multiplexed compound biosynthesis and will serve as a valuable tool for enhancing one-carbon (C1) bio-utilization.

1. Introduction

The precise and efficient gene editing system plays a significant role in metabolic engineering and synthetic biology. The clustered regularly interspaced short palindromic repeats/Cas9 (CRISPR/Cas9) system, a revolutionary genetic tool with precise targeting and markerless manipulation, has been widely used for gene editing in model microorganisms, including *Escherichia coli* and *Saccharomyces cerevisiae*. Although *Pichia pastoris* (syn. *Komagataella phaffii*) is not a model organism, its growing significance is attributed to its efficient methanol utilization capability in contemporary research and applications.

Currently, the CRISPR/Cas9 system has been optimized to increase targeting efficiency and reduce potential off-target effects in *P. pastoris* [1]. The targeting efficiency of neutral locus integration in *P. pastoris* has improved to nearly 100 % through the knockout of *ku70* (a non-homologous end joining gene) and the overexpression of *Rad52* (a homologous recombination-related gene) [2]. However, more rapid and efficient methods for functional gene disruption and multiple gene integration remain a bottleneck for metabolic engineering in *P. pastoris*, especially the one step approach for multi-gene editing. One crucial

* Corresponding author.
** Corresponding author.
*** Corresponding author.
E-mail addresses: bo.wang@siat.ac.cn (B. Wang), tao.yu@siat.ac.cn (T. Yu), sy.guo@siat.ac.cn (S. Guo).
[1] These authors contributed equally to this work.

https://doi.org/10.1016/j.synbio.2025.01.005
Received 9 August 2024; Received in revised form 13 December 2024; Accepted 15 January 2025
Available online 23 January 2025

component of the CRISPR/Cas9 system is the efficient expression of mature single-guide RNA (sgRNA), which comprises a 20-base pair gRNA sequence at the 5′-end, specifically targeting the genome, and a scaffold that activates Cas9 to cleave double-stranded DNA. Therefore, there is an urgent need to develop convenient tools and efficient methods for the high-throughput and high-efficiency expression of multiple sgRNAs to enable targeted multiplexed genome modification.

Typically, sgRNA is expressed by RNA polymerase III (Pol III) promoters such as U3 in plants, U6 in mammals and SNR52 in *S. cerevisiae*. The promoters usually express sgRNA with no additional base modification at the 5′-end to prevent misleading identification and pairing of target loci [3–5]. However, the use of combinations of RNA Pol III and Cas9 from different sources led to only a 31.7 % targeting efficiency for single gene disruption, indicating inefficient genome editing when sgRNA is directly expressed by RNA Pol III [6]. Furthermore, the universal utilization of RNA Pol III promoters across species is limited due to their constitutive nature and uniqueness to the host genome, which is characterized by limited conserved motifs [7,8]. Hence, only a few studies have reported genomic editing efficiencies in *P. pastoris*, with 80 % for *ade2* and 30 % for *gut1* [9].

The RNA polymerase II (Pol II) promoter, which is responsible for the production of the majority of mRNAs, exhibits strong transcriptional activity and offers spatially/temporally inducible control [10]. However, this approach has not been widely adopted for sgRNA expression because of transcribed premature sgRNAs with a cap structure at the 5′-end and a poly-A tail at the 3′-end, which negatively influence precise localization and functionality [10,11]. Therefore, to avoid extra modifications at the 5′-end and 3′-end, it is necessary to design and correct the processing of pre-sgRNA. The nuclease activity of ribozymes has been adopted to design a pre-sgRNA structure called RGR (Ribozyme-gRNA-Ribozyme), which includes a Hammerhead (HH)-type ribozyme at the 5′-end, a sgRNA in the middle, and a hepatitis delta virus (HDV) ribozyme at the 3′-end [12]. After transcription, the ribozymes self-cleaved at both ends, releasing the mature sgRNA without modifications. With this strategy, a series of RNA Pol II promoters, such as pTEF, pHTB1 and pGAP, have been characterized in *P. pastoris*, and the editing efficiency can reach 68 %–100 % [2,6,13,14]. Moreover, tRNA sequences were incorporated as spacers to fuse with several sgRNAs, and all the sgRNAs were transcribed into a single transcript. Subsequently, the endogenous tRNA processing system recognizes and cleaves tRNA at the 5′ and 3′ ends, releasing mature sgRNAs targeting multiple loci [15]. The use of a gRNA-tRNA array enabled the simultaneous disruption of 8 genes in *S. cerevisiae* with 87 % efficiency [16], while limited research has been conducted in *P. pastoris*. Therefore, we can establish a high-throughput mature sgRNA system by screening the optimal processing of pre-sgRNAs to achieve simultaneous multiple genomic editing in *P. pastoris*.

In this study, we aimed to construct a rapid and convenient multigene editing system to enable one-step complex metabolic engineering in *P. pastoris*. Considering that the impact of sgRNA processing strategies on the efficiency of genetic engineering, we constructed three different sgRNA processing cassettes in *P. pastoris* promoted by RNA Pol II, which contained a tRNA-sgRNA-tRNA (tgt) array, HH-sgRNA-HDV (HgH) structure and their combination, and compared the gene disruption efficiency in terms of single/double gene deletion, double-locus disruption and integration respectively. We demonstrated that the HgH structure had the highest efficiency both in single-gene and dual-gene knockouts (Table 1). Furthermore, we successfully applied this system for one-step biosynthesis of free fatty acids (FFAs) and 5-hydroxytryptophan (5-HTP), which significantly reduced the time required to construct target engineered strain and improved the overall efficiency. We believe this system can facilitate multiplexed metabolic engineering in *P. pastoris* in the future.

2. Results

2.1. Design of a single gene deletion system for releasing mature gRNAs

In our preliminary study, we successfully constructed a HiEE-ReSM system with high editing efficiency in *P. pastoris,* which contained an HR-enhanced platform strain GSY002 (*Δku70::Rad52-Rad59*, Supplementary Table 3), and the positive rate reached 97 % compared to that of the basal strain GS115 [14]. However, its multiplexed application is still limited by its guide RNA (gRNA) processing efficiency and throughput. To improve its ability required for multi-deletion of functional genes and multi-locus integration, we first optimized the expression of the sgRNA.

We also selected the plasmid pBB3cH_pGAP_23_pLAT1_Cas9, which can express elemental gRNA *via* the GAP promoter, a type of RNA Pol II promoter, as the base vector. Then, we designed three sgRNA processing cassettes: (i) tRNA-gRNA-tRNA (named tgt), (ii) tRNA-gRNA-HDV (named tgH), and (iii) HH-sgRNA-HDV (named HgH). The fragments in the cassettes were constructed by overlap extension PCR (OE PCR) using the primers listed in Supplementary Table 5. *Bbs*I recognition sites were introduced at both ends of each fragment. Specifically, the fusion site at the 3′-end of the preceding fragment and the 5′-end of the following fragment was established by incorporating the first four nucleotides from the 20-base pair gRNA sequences. After the fragments were assembled into the base vector, the primary gRNAs were expressed by the GAP promoter. Finally, the mature gRNAs were released through self-cleavage or endogenous RNase-mediated cleavage (Fig. 1A).

In detail, the first cassette, named "tgt", consisted of a central gRNA flanked by tRNA on both sides. We chose $tRNA^{Gly}$ from *S. cerevisiae* for gRNA processing because it has been successfully applied to process gRNA in plants [17], mammalian cells [10], zebrafish [18], and the model yeast strain *S. cerevisiae* [16]. To prevent mis-fusion due to repetitive tRNA sequences, we divided the "tgt" cassette into two fragments. One fragment contained $tRNA^{Gly}$, and the other contained sgRNA-$tRNA^{Gly}$. The second cassette, named "tgH", included $tRNA^{Gly}$ upstream and HDV ribozyme downstream of gRNA. Similar to the "tgt" cassette, two fragments were designed to construct the "tgH" cassette with one $tRNA^{Gly}$ fragment and another sgRNA-HDV fragment. The third cassette, named "HgH", contained an HH ribozyme at the 5′-end and an HDV ribozyme at the 3′-end of gRNA, which consists of only one segment. The first six nucleotides (in green or pink) of the Hammerhead (HH) ribozyme must be complementary to the first six nucleotides of the 20 bp target sequence (in green or pink), which together formed the Hammerhead (HH) structure [12]. Mature gRNAs without modifications

Table 1
Comparison of HiEE-ReSM (original) system and new system in this study.

	gRNA processing strategy	Single disruption efficiency		Double disruption efficiency		Improvement
		Functional gene	Neutral site	Functional genes	Neutral sites	
HiEE-ReSM system	HH/HDV	Not detected	100 % for II-4	Unable	Unable	Homologous enhancement compared to GS115
This study	tRNA, tRNA/HDV, HH/HDV	95.8 % for *Δgut1*, 89.6 % for *Δaox1*	Not detected	59.7 % for *Δaox1Δgut1*, 57.1 % for *Δfaa1Δfaa2*	100 % for II-4/II-5	Application expansion to double disruption, screening HH/HDV as the most optimal gRNA processing

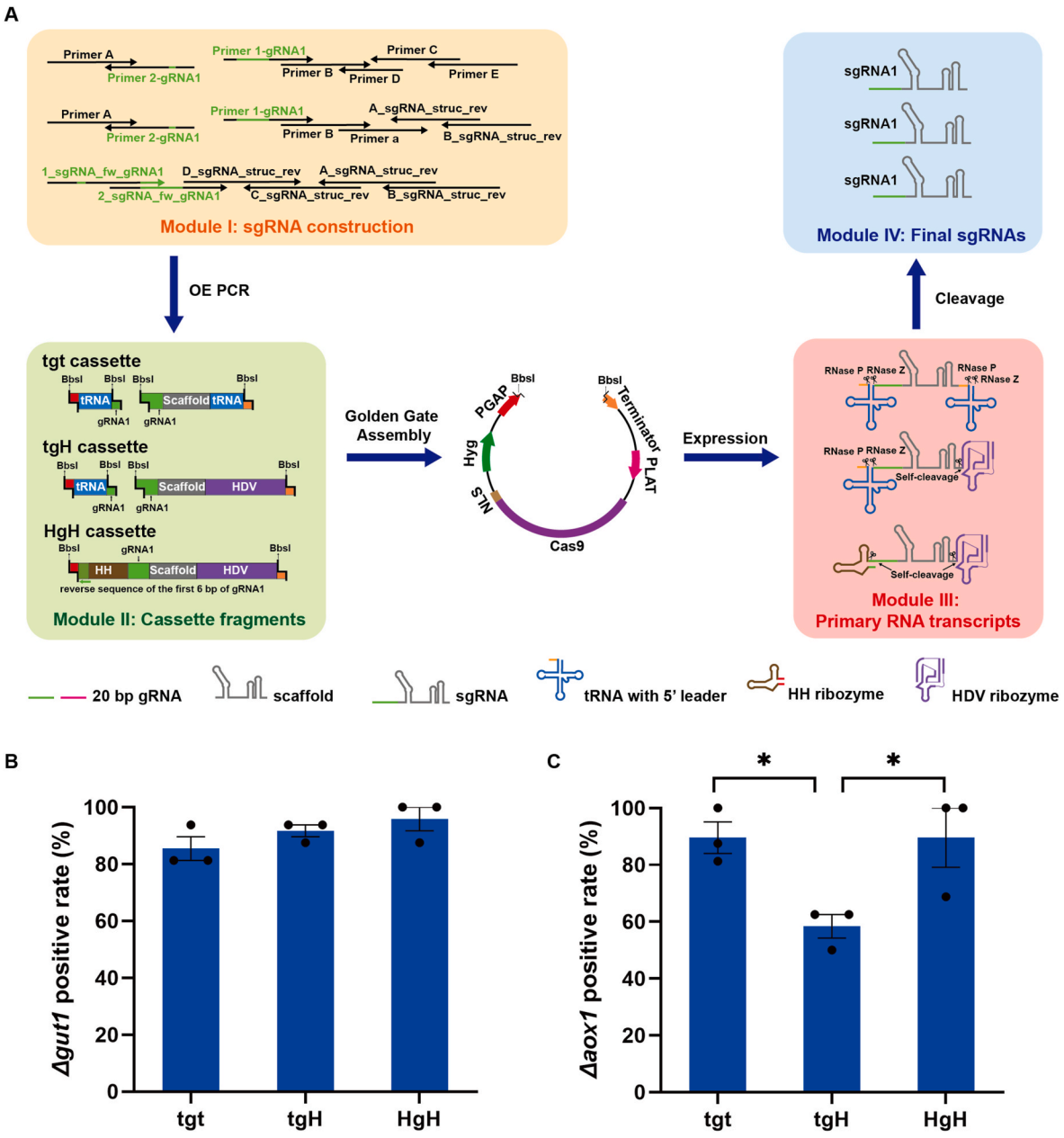

Fig. 1. Construction and evaluation of three single-gene deletion systems.
A. The workflow diagrams of three single-gene sgRNA processing cassettes in *P. pastoris*. In detail, fragments conforming three sgRNA expression cassettes can be obtained through fusion PCR. *Bbs*I recognition sites were introduced at both ends of each fragment. The sites marked in red and orange would fuse with the vector, and the sites marked in green would fuse together to conform a complete sgRNA sequence. Then, all three sgRNA cassettes were assembled into vectors *via* Golden Gate cloning. After transformation into yeast cell, pre-sgRNA was expressed. Finally, pre-sgRNA was processed and released mature sgRNA. The tgt, tgH and HgH cassettes represent the structures of tRNA-sgRNA-tRNA, tRNA-sgRNA-HDV and HH-sgRNA-HDV, respectively.
B–C. The positive rates of the *Δgut1* (B) and *Δaox1* (C) transformants identified on the upstream and downstream sides.
The error bars indicate the standard deviations of three biological replicates. Each black dot represents 16 colonies. The data were analysed by an unpaired two-tailed Student's *t*-test. $*p < 0.05$.

were released after cleaving the $tRNA^{Gly}$ or HH-HDV ribozyme. Specifically, $tRNA^{Gly}$ is cleaved at the 3′-end by RNase Z and at the 5′-end by RNase P. Meanwhile, the HH ribozyme self-clears at the 3′-end, and the HDV ribozyme self-clears at the 5′-end [12,15].

To verify and compare the three sgRNA processing cassettes, we chose glycerol kinase 1 (GUT1) and alcohol oxidase 1 (AOX1) to test single gene disruption efficiency. The sgRNAs we chose have been confirmed of high efficiency in previous study [6]. Sixteen transformants were randomly selected from each of three biological replicates, and a total of 48 colonies were selected from each cassette. For verification upstream and downstream of the target gene, successfully edited transformants were subjected to a 1 kb band on a 1 % agarose gel. For *gut1* disruption, nearly all the selected colonies were correct, with positive rate of at least 85 % and up to 95 % (Fig. 1B). The targeting efficiencies were 95.8 %, 91.7 %, and 85.4 % for cassette HgH, tgH, and tgt, respectively, and no significant differences were observed among them. However, for *aox1* disruption, the positive percentage ranged from 58.6 % for tgH to 89.6 % for tgt and HgH, which exhibited slightly lower efficiency than *Δgut1* especially on tgH (Fig. 1C). This may be attributed to the differences of gene.

In conclusion, gRNA flanked with either $tRNA^{Gly}$ or HH/HDV ribozymes could be processed precisely and effectively guide Cas9 break target genes with high efficiency.

2.2. Expanding the expression cassette of mature gRNAs for simultaneous disruptions at double loci

Based on the high efficiencies of the three cassettes for gRNA processing, we expanded them for double gene disruptions. The cassette structure was like that used for single gene deletion, and *Bbs*I recognition sites were incorporated at both ends of each fragment. Specifically, for dtgt (double tgt) cassettes, each gRNA was flanked with $tRNA^{Gly}$ on both sides to form a tRNA-gRNA1-tRNA-gRNA2-tRNA structure. The cassette was divided into three fragments, with the first fragment containing tRNA, the second containing gRNA1-tRNA, and the third containing gRNA2-tRNA. The first four nucleotides of gRNA1 were set as the fusion site between the first and second fragments, and the first four nucleotides of gRNA2 were set as the fusion site between the second and third fragments. For the dtgH (double tgH) cassette, three fragments contained tRNA, gRNA1-HDV-tRNA, and gRNA2-HDV-tRNA. The sets of fusion sites used were the same as those used for the dtgt cassette. The dHgH (double HgH) cassette was split into two fragments, each containing a sgRNA flanked by HH and HDV ribozymes. The first four nucleotides of the HH ribozyme sequence were set as the fusion site between the front fragment and the following fragment (Fig. 2A).

We selected *gut1* and *aox1* to verify the efficiency of double disruption. Originally, we arranged the *gut1* sgRNA in front of the *aox1* sgRNA. As a result, we found that the strain growth was significantly impaired, for the number of transformants was lower than that observed in single gene deletion, such as only 45 clones from dHgH being the least. This

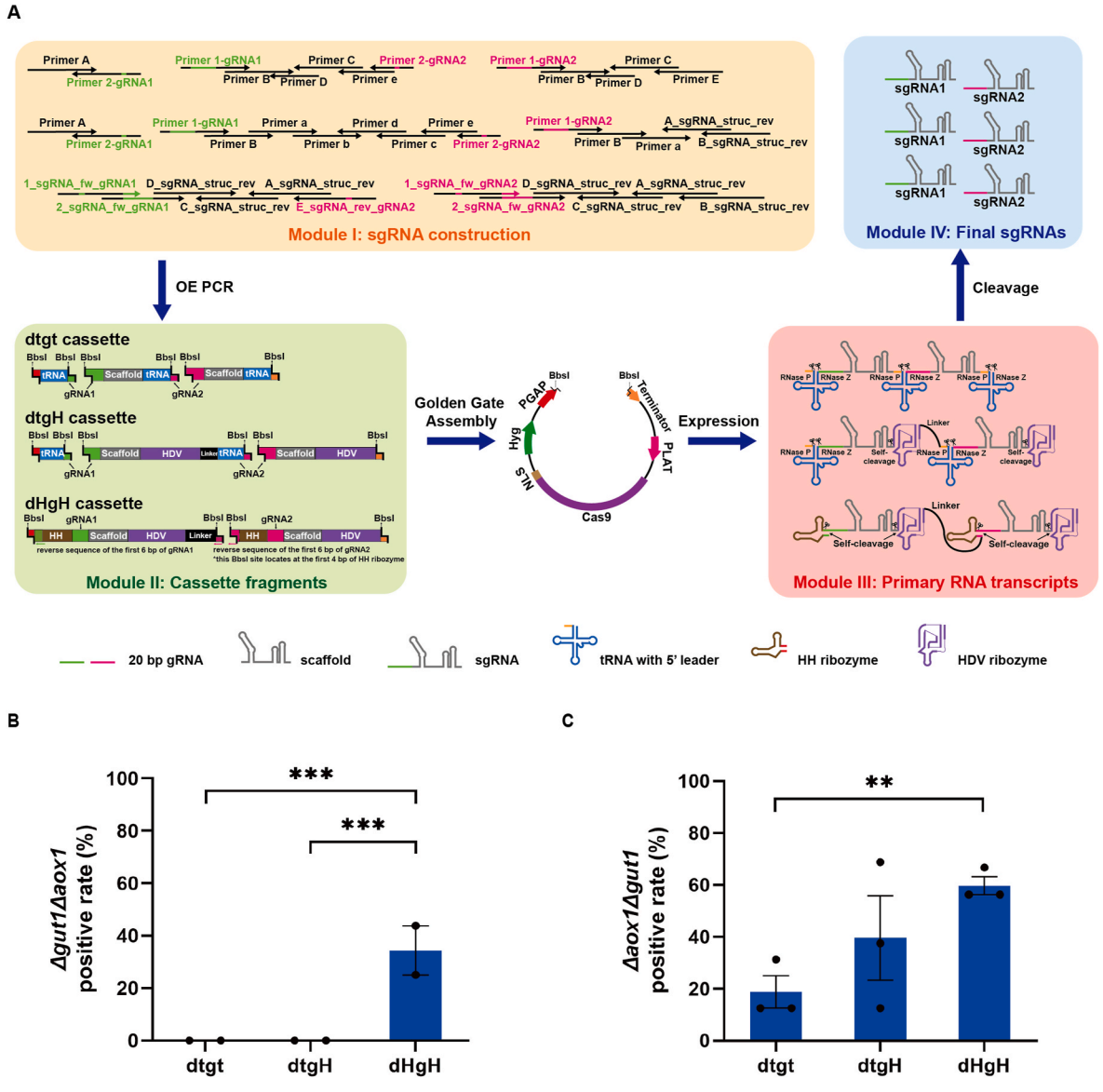

Fig. 2. Three cassettes for double-gene sgRNA processing in *P. pastoris*.
A. The workflow diagrams for one-step construction of three dual-gene sgRNA processing cassettes in *P. pastoris*. The detailed operating method was as the same as single-gene sgRNA processing cassettes. Specially, *Bbs*I sites marked in green or pink of dtgt and dtgH cassettes would fuse together to conform a complete sgRNA sequence, and sites marked in pink of dHgH cassette would fuse together to conform a complete HH ribozyme sequence. The dtgt, dtgH and dHgH cassettes represent the structures of tRNA-sgRNA1-tRNA-sgRNA2-tRNA, tRNA-sgRNA1-HDV-tRNA-sgRNA2-HDV and HH-sgRNA1-HDV–HH–sgRNA2-HDV, respectively.
B–C. The positive rates of the *Δgut1Δaox1* (B) and *Δaox1Δgut1* (C) transformants identified on the upstream and downstream sides.
The error bars indicate the standard deviations of two or three biological replicates. Each black dot represents 16 colonies. The data were analysed by an unpaired two-tailed Student's *t*-test. $^{**}p < 0.01$, $^{***}p < 0.001$, **ns**: no significance.

may be due to the lethality of inefficient repair at any DSB site. Additionally, the cultivation time was extended from 3 days to 5 days, suggesting that the repair and growth of double knockout-positive colonies occurred more slowly compared to single gene deletion strains. As for editing efficiency, only dHgH cassette achieved 34.4 % positive rate for *Δgut1Δaox1*, while no positive transformants was obtained for double gene disruption in dtgt and dtgH cassette (Fig. 2B). Specially, we observed a significant difference in the incomplete double-knockout (only *gut1* was disrupted or only *aox1* was disrupted) percentage. In the double knockout plate of *Δgut1Δaox1*, only transformants with a single *Δgut1* were obtained, ranged from a minimum of 40.6 % to a maximum of 93.8 % in three sgRNA cassettes (Table 2), while no transformants with a single *Δaox1* knockout were found, which may be attributed to the differences of gRNA sequences, gRNA positions, and genes' heterogeneity. Since the same gRNA sequence of *Δaox1* has been successfully applied in the previous section for single *Δaox1* (Fig. 1C), we initially ruled out the gRNA sequence itself was a contributing factor. To assess the impact of gRNA positions on editing efficiency, we placed the *aox1* sgRNA in front of *gut1* sgRNA to verify editing efficiency. Surprisingly, the results exhibited that dual knockout efficiencies of all three cassettes were improved, with 18.58 %, 39.4 % and 59.7 % for dtgt, dtgH and dHgH, respectively (Fig. 2C). This suggested that the order of sgRNAs significantly influences the overall double-knockout efficiency. Additionally, the percentage of single *Δgut1* knockout decreased significantly, reaching a maximum of only 10.4 %. This may be due to the sgRNA being positioned farther from the promoter, resulting in lower expression and editing efficiency. Even though the *aox1* sgRNA was swapped first, the single-knockout efficiency remained only 2.1 %, showing no significant improvement. This result indicates that gene heterogeneity has a greater impact on efficiency during multi-gene knockouts (Table 2). To further assess the differences of three sgRNA cassettes on multi-gene knockout efficiency, we also selected another gene, phosphoribosylaminoimidazole carboxylase 2 (ADE2), and tested the efficiency of *Δgut1Δade2* double knockout. The sgRNA targeting *gut1* was the same as that used for *Δgut1Δaox1*, and the *ade2* sgRNA had previously been reported to exhibit high editing efficiency [9]. Only the dHgH structure successfully achieved dual knockouts among three cassettes, with an efficiency of 16.7 % for *Δgut1Δade2* (Supplementary Table 1). The result further confirmed the conclusion that dHgH was the most optimal choice for dual gene deletion, and the contrast between *Δgut1Δaox1* and *Δgut1Δade2* also suggested that the efficiency of double knockouts was influenced by the specific genes targeted.

In summary, the dHgH cassette performed the best performance in double-gene deletion the among the three sgRNA processing designs.

2.3. Application of the dHgH system for fatty acid production in *P. pastoris*

After confirming the effectiveness of the three sgRNA processing strategies for double-gene disruption, we applied the best dHgH cassette for production of free fatty acids (FFAs). FFAs are energy-rich lipids that are structural components of cell membranes. Recently, the engineering of FFAs and their derivatives has garnered significant attention as a renewable route for producing high-energy-density biofuels and valuable oleochemicals [19]. FFAs can be synthesized *de novo* from methanol through a three-step process in *P. pastoris*. First, methanol can be oxidized to formaldehyde and hydrogen peroxide, and formaldehyde is assimilated into central carbon metabolism through the xylulose monophosphate (XuMP) pathway, where xylulose 5-phosphate (Xu5P) can serve as a formaldehyde acceptor to generate glycerol aldehyde-3-phosphate (G3P) and dihydroxyacetone (DHA) *via* dihydroxyacetone synthase (DAS). Furthermore, DHA can be converted to G3P through dihydroxyacetonephosphate (DHAP). In the second step, acetyl-CoA, which serves as the precursor for FFAs formation, is derived from G3P through the classical steps of glycolysis. In the end, FFAs can be synthesized through the hydrolysation of fatty acyl-CoAs by thioesterase (TesA), which can be formed through the condensation of acetyl-CoA and malonyl-CoA by fatty acid synthase (FAS). Notably, FFAs can be rapidly reactivated by fatty acyl-CoA synthetases (FAA) and converted back to fatty acyl-CoAs in wild-type strains [20]. Therefore, for the FFA-producing phenotype, disruption of genes *faa1* and *faa2* is

Table 2
Overview of all knockout results.

Disruption locus	Repair fragments	Repair fragment length	gRNA processing strategy	Identified clones	Single knockout efficiency	Double knockout efficiency
Δgut1	GUT1up-GUT1dn	1 kb	tgt	16	85.4 %	/
			tgH	16	91.7 %	/
			HgH	16	95.8 %	/
Δaox1	AOX1up-AOX1dn	1 kb	tgt	16	89.6 %	/
			tgH	16	58.63 %	/
			HgH	16	89.6 %	/
Δgut1Δaox1	GUT1up-GUT1dn AOX1up-AOX1dn	1 kb, 1 kb	dtgt	16	56.3 % for *Δgut1*, 0 % for *Δaox1*	0 %
			dtgH	16	93.8 % for *Δgut1*, 0 % for *Δaox1*	0 %
			dHgH	16	40.6 % for *Δgut1*, 0 % for *Δaox1*	34.4 %
Δaox1Δgut1	GUT1up-GUT1dn AOX1up-AOX1dn	1 kb, 1 kb	dtgt	16	8.3 % for *Δgut1*, 2.1 % for *Δaox1*	18.75 %
			dtgH	16	10.4 % for *Δgut1*, 2.1 % for *Δaox1*	39.4 %
			dHgH	16	0 % for *Δgut1*, 2.1 % for *Δaox1*	59.7 %
Δfaa1Δfaa2	FAA1up-FAA1dn FAA2up-FAA2dn	1 kb, 1 kb	dHgH	14	None of single disruption	57.1 %
	FAA1up-*GPM1p-TesA-ADH1t*-FAA1dn FAA2up-*GPM1p-TesA-ADH1t* -FAA2dn	2.3 kb, 2.3 kb	dHgH	14	None of single disruption	14.3 %
	FAA1up-*GAPp-fas1-PMP20t*-FAA1dn FAA2up-*ADH1t-TesA-GPM1p-PGIp-fas2-DAS1t*-FAA2dn	8 kb, 8.5 kb	dHgH	14	None of single disruption	0 %
II-4 II-5	II-4up-*GAPt-mut-tph-GAPp-TEF1p-pts-DAS1t*-II-4dn II-5up-*GAPt-spr-GAPp-TEF1p-gch1-DAS1t*-II-4dn	3.9 kb, 4 kb	dHgH	9	None of single disruption	100 %

necessary, and over expression of gene *TesA, fas1* and *fas2* would further increase the titre of FFAs (Fig. 3A). Generally, double-gene knockout and triple-gene insertion would require at least two steps. However, our system allows for the one-step construction of a phenotype for fatty acid production by simultaneously knock out *faa1/faa2* and integrate three types of repair fragments to increase the production of FFAs. The first strain, K001, contained only 1000 bp homologous arms. The second one, named K002, contained two copies of *TesA* according to studies by Zhou [20] with 1000 bp homologous arms, and strain K003 contained one copy of *TesA* and one copy of *fas1* and *fas2* amplified from the *P. pastoris* genome with 1000 bp homologous arms (Fig. 3B).

For the double-deletion transformants, 8 out of 14 colonies were positive for K001, with an editing efficiency of 57.1 %, and 2 out of 14 colonies were positive for K002, with an efficiency of 14.3 %. Unfortunately, no K003-positive colonies were obtained (Table 2). This may be attributed to two reasons: 1) the efficiency of insertion at functional genes was lower than neutral sites integration, while FFA pathways in K003 were inserted at functional genes; 2) as the length of inserted fragments increases, the integration efficiency would significantly decrease, which has been demonstrated in previous study [21,22]. Finally, we detected FFAs production in K001 and K002; 20.2 mg/L/μg protein/OD FFAs were produced by K001, and the titre of K002 was 23 mg/L/μg protein/OD, while nearly no FFAs were detected in strain GSY002, which confirmed that *faa1* and *faa2* were successfully disrupted in strains K001 and K002. Regrettably, no significant differences in the FFAs titre were observed between K001 and K002, despite the slightly greater production of FFAs in K002, which suggested that the overexpression of *TesA* alone did not lead to an increase in FFAs production.

Overall, the production of FFAs from methanol demonstrated the feasibility and potential of the dHgH cassette for double deletion and double integration in the *P. pastoris* genome.

2.4. Application of the dHgH system for 5-hydroxytryptophan production in P. pastoris

Multi-integration of functional genes is necessary for cell factory construction, to evaluate the efficiency of dHgH for multi-gene integration, four genes for 5-hydroxytryptophan (5-HTP) synthesis were designed to insert into two neutral sites II-4 and II-5 at the same time. 5-HTP is a high-value pharmaceutical product which participates in the regulation of human physiological activities and plays an important role in the clinical treatment of depression, insomnia, obesity and migraine [23]. For 5-HTP synthesis, tryptophan is hydroxylated one-step by tryptophan hydroxylase (TPH), in which tetrahydrobiopterin (BH4) performs as a critical cofactor providing two electrons for reduction [24]. BH4 can be synthesized *de novo* from methanol through a three-step process. Firstly, ribose-5-phosphate (R5P) is generated

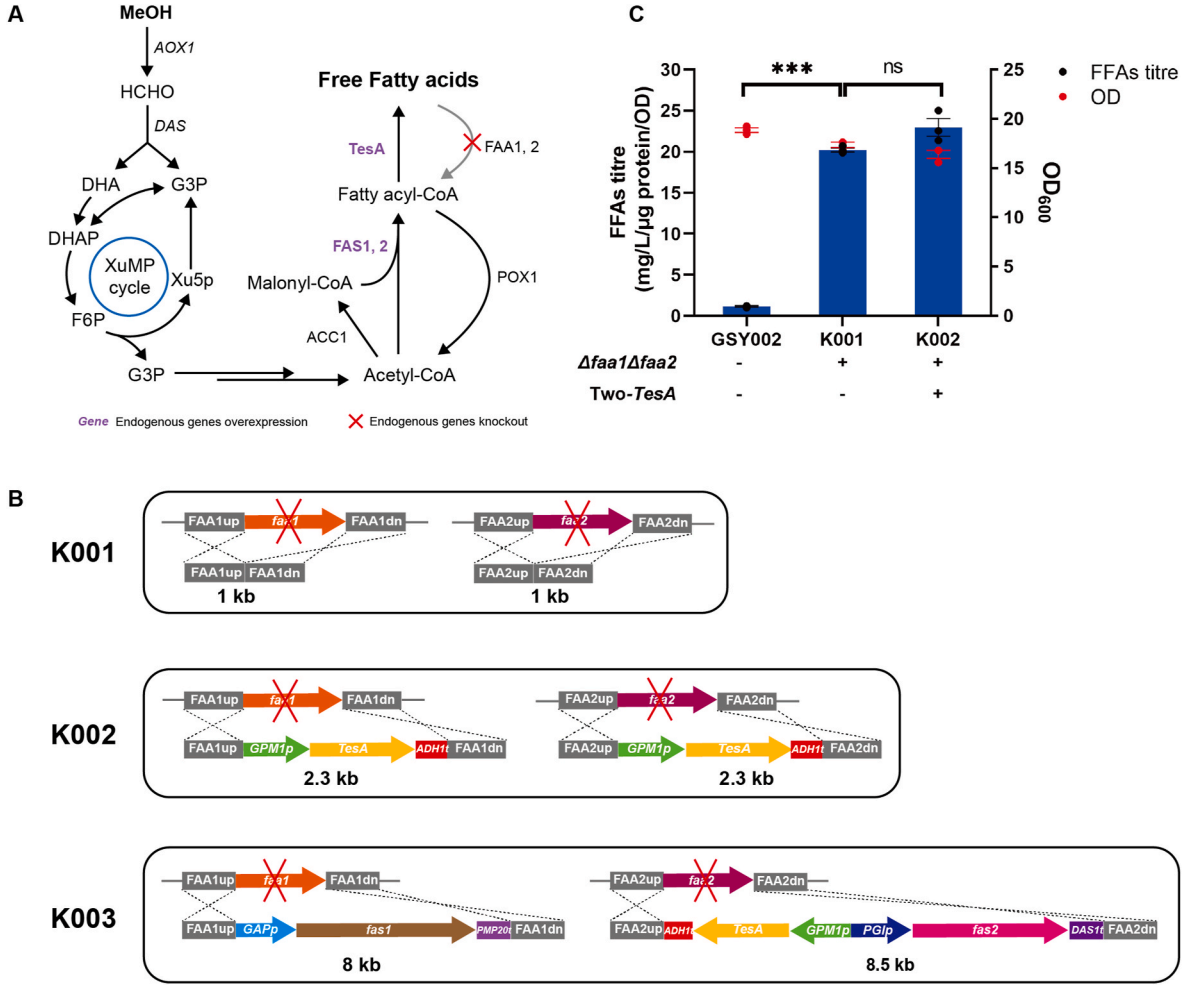

Fig. 3. One-step construction of the free fatty acids production phenotype in *P. pastoris*.
A. The biosynthetic pathways of FFAs production in *P. pastoris*.
B. Repair fragments designed for constructing strains K001, K002 and K003.
C. The titre of FFAs in strains K001 and K002 was measured in shake flasks. The error bars indicate the standard deviations of three biological replicates. The data were analysed by an unpaired two-tailed Student's *t*-test. ***$p < 0.001$, **ns**: no significance.

through XuMP cycle and pentose phosphate pathway from methanol. Secondly, R5P undergoes 15 enzymatic reactions and converts to guanosine triphosphate (GTP) [25,26]. At last, BH4 can be synthesized by sequential catalysis of GTP by endogenous GTP cyclohydrolase 1 (GCH1), exogenous 6-pyruvoyl-tetrahydropterin synthase (PTPS) and sepiapterin reductase (SPR) [27]. Therefore, to establish a 5-HTP-producing strain K004, several exogenous genes for tryptophan hydroxylation and cofactor BH4 synthesis must be introduced simultaneously. Using the one-step integration approach with the dHgH cassette can significantly save time in achieving this goal. In this study, truncated human TPH2 (NΔ145/CΔ24) with E2K, N97I and P99C mutations (mut-TPH) and BH4 synthesis pathway from *Rattus norvegicus* were both introduced into *P. pastoris* (Fig. 4A) [28,29]. We designed two repair fragments of similar length, with one contained *mut-tph* and *pts* for II-4 neutral site integration, and another contained *spr* and one copy of endogenous *gch1* for II-5 neutral site, both of which were flanked with 1000 bp homologous arms (Fig. 4B).

For the result, transformant numbers were much more than *Δgut1Δaox1* and *Δfaa1Δfaa2* double-disruption, with colonies overgrew full of the plate. Besides, the positive rate for insertion at double loci among nine colonies randomly selected was 100 %, demonstrating the high efficiency of dHgH for multi-gene integration. Afterwards, 5-HTP production was detected with methanol as the carbon source. However, no significant growth of K004 was observed on the third day of fermentation, which may be that the constitutive synthesis of BH4 consumed much energy and GTP which affected the utilization of methanol [30,31]. To provide the initial energy for methanol assimilation, 0.125 % glycerol was added to the media. Finally, 13.3 mg/L 5-HTP was detected in strain K004.

In conclusion, the 100 % editing efficiency and 5-HTP production from methanol demonstrated the high availability of the dHgH cassette for simultaneous integration of multi-gene at double locus in *P. pastoris*.

3. Discussion

With the continually declining global price of methanol, *P. pastoris* has attracted increasing interest for developing a promising and versatile platform chassis for multiplex chemical production due to its efficient methanol utilization capability, which has promoted the demand for the development of more efficient gene editing tools based on the CRISPR/Cas9 system. Given the critical role of pre-sgRNA processing in editing efficiency, we focused on identifying the optimal strategy for processing pre-sgRNAs to enable convenient and efficient simultaneous multi-genomic editing in *P. pastoris*. Our results showed that the HH-sgRNA-HDV structure outperformed the other two sgRNA processing cassettes tRNA-sgRNA-tRNA and tRNA-sgRNA-HDV in terms of both single and double knockout efficiency. Additionally, we successfully applied the HH-sgRNA-HDV structure for one-step biosynthesis of fatty acids and 5-HTP.

Several strategies have been explored to enhance the efficiency and throughput of sgRNA expression, including the use of ribozymes and tRNAs. HH and HDV ribozymes were primarily employed, while fewer systems were related to tRNA in *P. pastoris.* Therefore, we first selected *gut1* and *aox1* as the demo gene to validate the efficiency of single-locus deletion by constructing the HH-sgRNA-HDV cassette. We achieved a relatively higher positive rate of 95.8 %, aligning with other reports that used the HH/HDV structure but employed different promoters (pHTX1 or pHTB), with reported ranges spanning from 68 % to 90 % [2,6]. The tRNA-based system, which uses endogenous tRNA processing machinery, has been applied in the model yeast *S. cerevisiae* and is able to express up to 8 gRNAs simultaneously [16]. Hence, the design of tRNA flanking cassette for *gut1* or *aox1* knockout, achieving an efficiency of

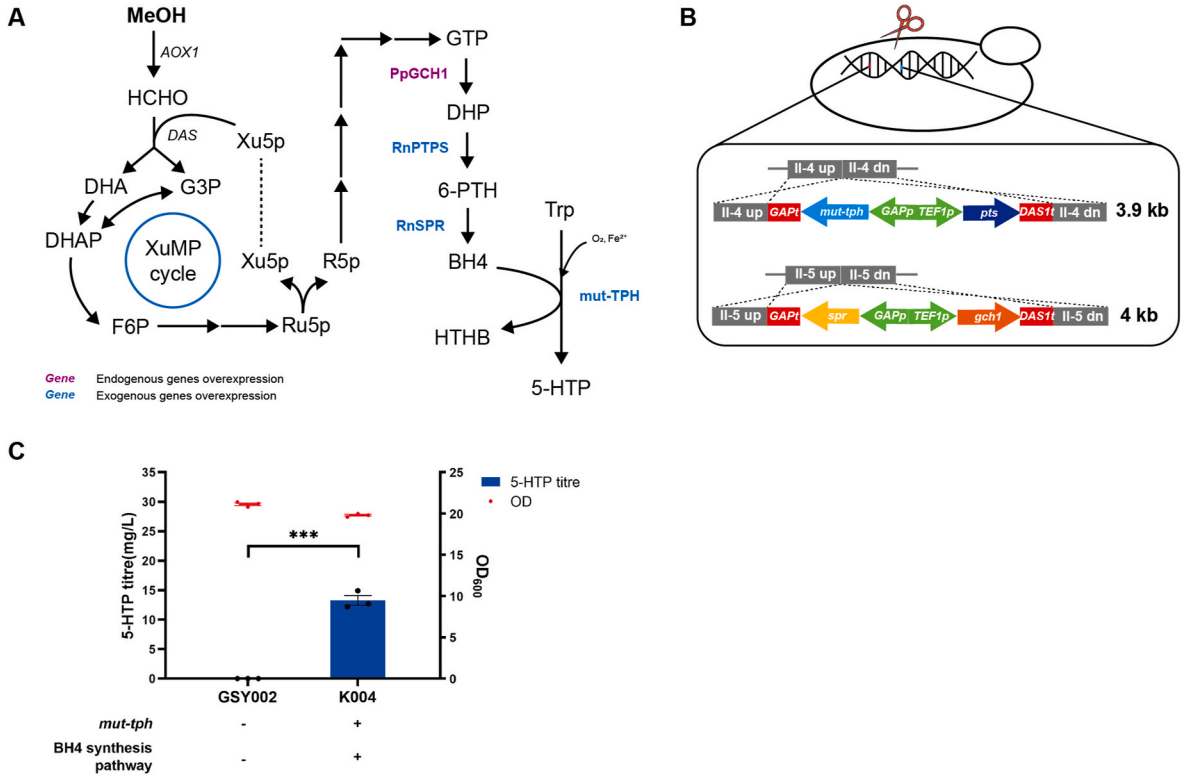

Fig. 4. One-step construction of the phenotype to produce 5-hydroxytryptophan in *P. pastoris*.
A. The biosynthetic pathways of 5-HTP production in *P. pastoris*.
B. Repair fragments designed for constructing strains K004.
C. The titre of 5-HTP in strain K004 was measured in shake flasks. The error bars indicate the standard deviations of three biological replicates. The data were analysed by an unpaired two-tailed Student's *t*-test. ***$p < 0.001$, **ns**: no significance.

85.4 % or 89.6 % in *P. pastoris* through the HR repair system. This percentage was slightly lower than that in a previous study, which reported a 90 % positive rate for *och1* deletion and a 100 % positive rate for *ku70* deletion using NHEJ [32]. We attribute these differences mainly to gene-specific characteristics. Considering the problems of potential excess nucleotides attached to the sgRNA flanked by tRNA at the 3′-end and the complicated cloning process required for HH ribozymes at the 5′-end, which must match the first six nucleotides of the gRNA targeting sequence, we designed a tRNA-sgRNA-HDV cassette. Although this design had not been previously employed in *P. pastoris*, it exhibited an impressive positive rate of 91.7 % for *Δgut1* and 58.6 % for *Δaox1*. To date, all the three different gRNA processing cassettes demonstrated high availability and efficiency in single gene disruption.

Currently, for multi-locus deletions of functional genes, only two studies have reported related results in *P. pastoris*. One study achieved a positive rate of 69 % for removing *gut1* and *aox1* at the same time using NHEJ [6], while the other reached 86.7 % for *faa2/hfd1* double disruption using HR [13]. Both studies selected the HH/HDV structure and expressed gRNA with pHTX1 promoter (Table 3). We used the three cassettes to simultaneously disrupt two functional genes, *gut1* and *aox1*. In our study, placing the *aox1* sgRNA at the front resulted in successful double deletions with all three cassettes. Furthermore, this adjustment increased the positive rate of the best-performing dHgH cassette from 34.4 % to 59.7 %, highlighting the significant impact of sgRNA order on overall editing efficiency. However, this positive rate remains lower than previously reported values. Compared to the other two studies, we speculate that the discrepancy of double gene disruption can be attributed to three reasons. The first reason is the significant difference in the HR efficiency of the chassis cell. According to the study of Zhang et al., the positive rates for simultaneous seamless deletion of two genes and three genes can be improved by fusing MRE11 (exonuclease) to the C-terminus of CAS9 and overexpressing *Rad52* [13], but our chassis cell lacks further genetic modifications to the homologous recombination system. Second, the low positive rate may be attributed to the heterogeneity between functional genes and gRNA sequences targeting the same gene. In our study, we achieved various efficiencies of double-locus disruption, with the lowest 18.75 % for *Δaox1Δgut1* and up to 100 % for II-4/II-5 (Table 2). Moreover, the efficiencies of individual gene in double-locus disruption ranged from 0 % for *Δaox1* to 93.8 % for *Δgut1*, which was also observed in other studies, where the percentage of positive strains increased from 30 % for *Δgut1* to 100 % for *Δku70* [9,32]. Moreover, differences in targeting efficiency can occur even for the same gene. In a previous study, the disruption efficiency of three gRNAs varied from 5 % to 94 %. Because some gRNAs may incorrectly bind to Cas9 due to specific RNA folding, certain target sequences may be inaccessible to the nuclease due to chromatin status [6]. Finally, episomal plasmids, including the autonomously replicating sequence (ARS) and the promoter of gRNA, are believed to be associated with knockout efficiency. The ARS from *Kluyveromyces lactis* has been widely utilized in plasmids and exhibited two-fold greater stability, transformation efficiency and copy numbers than the ARS from *S. cerevisiae* in this study [9]. The positive rates are also related to the type of promoter used for gRNA expression, including RNA Pol II and RNA Pol III. Furthermore, some studies have shown that variations in the promoter of gRNA may lead to poor mutation rates, in contrast to other studies in which the efficiency approaches 100 % [6,13,33]. Therefore, we can improve multigene deletion efficiencies by improving HR frequencies, screening more gRNA sequences to target genes, and optimizing plasmid vectors, including but not limited to the promoters of gRNAs and ARS. Additionally, we speculate that the structure of the dtgt and dtgH cassettes may affect gRNA binding to the Cas9 protein, leading to the inactivation of dsDNA breaks and a high rate of off-target effects [8].

As for multi-locus gene integration, several research have been conducted at neutral sites. Therefore, to test the efficiency of dHgH on multi-integration, we applied dHgH on II-4/II-5 double neutral sites and achieved 100 % positive rate for K004 construction, which was much

Table 3
The CRISPR/Cas9-mediated gene editing system used in *P. pastoris*.

Based host	Repair system	gRNA processing strategy	Plasmid	Promoter for gRNA	Targeting Efficiency	Reference
The CRISPR/Cas9-mediated functional gene disruption in *P. pastoris*						
P. pastoris CBS 7435	NHEJ	HH/HDV	pPpT4 with PARS	pHTB (II)	94 % for *gut1* single disruption, 69 % ± 13 % for *gut1/aox1* double disruption	2016 [6]
P. pastoris GS115	HR	None	pPIC9K with panARS	pSER (III)	80 % for *ade2* single disruption and 30 % for *gut1* single disruption	2019 [9]
P. pastoris CBS 7435	NHEJ	tRNA	R_C2_gRNAgut1_kan	P_{tRNA1}	95 % for *gut1* single disruption, 40 % for triple integration	2020 [8, 32]
P. pastoris GS115	NHEJ	tRNA	pCas9 with PARS	P_{tRNA1}	93 % for *och1* single disruption, and 100 % for *ku70* single disruption	2021 [8, 32]
P. pastoris GS115-*PpRAD52*	HR	HH/HDV	pPICZ with panARS	pHTX1 (II)	68–90 % for *gut1* single disruption	2021 [2]
P. pastoris GS115-*RAD52*	HR	HH/HDV	pPICZ with panARS and Cas9 fused with exonuclease	pHTX1 (II)	91.7 % for *faa1* single disruption, 86.7 % for *faa2/hfd1* double disruption and 16.7 % for *faa2/hfd1/pox1* triple disruption	2022 [13]
P. pastoris GS115 *ΔKU70:RAD52-RAD59*	HR	tRNA, tRNA/HDV, HH/HDV	pBB3cH with cenARS	pGAP (II)	95.8 % for *gut1* single disruption and 59.7 % for *aox1/gut1*double disruption	This study
The CRISPR/Cas9-mediated neutral site integration in *P. pastoris*						
P. pastoris GS115 *ΔKU70*	HR	HH/HDV	pPIC3.5K with PARS	pHTX1 (II)	57.7 %–70 % and 12.5 %–32.1 % for double and triple-locus integration at upstream of *aox1/tef1/fld1* promoters	2019 [34]
P. pastoris GS115-Cas9	HR	None	pPIC9K with panARS	pSER (III)	~100 % for Int1 integration, ~93 % for Int1 and Int12 integration, and ~75 % for Int1, Int21 and Int12 integration	2022 [33]
HR efficiency enhanced *P. pastoris* GS115-Cas9-*RAD52-RAD59-MRE11*	HR	None	pPIC9K with panARS	pSER (III)	~100 % for Int1 integration, ~98 % for Int1 and Int12 integration, and ~81 % for Int1, Int12 and Int21 integration respectively with ~40 bp homology arms	2022 [35]
P. pastoris GS115 *ΔKU70:RAD52-RAD59*	HR	tRNA, tRNA/HDV, HH/HDV	pBB3cH with cenARS	pGAP (II)	100 % for II-4 and II-5 integration	This study

higher than simultaneous disruptions of functional genes. We speculated that this difference arises because the disruption at neutral sites has less impact on cellular physiology and metabolism than functional gene, which likely speed up the process of homologous recombination repair. This result was significantly higher than a previous study, where the efficiency ranged from 57.7 % to 70 % for double locus disruption [34]. The improved efficiency in our study might be attributed to the overexpression of RAD52 and RAD59, which enhanced homologous recombination (HR) efficiency, as well as the use of the GAP promoter for gRNA expression, which proved more effective in our system. Besides, the dHgH cassette in our study has slight advantage over the work of Gao et al., in which Pol III promoter pSER and panARS were used achieving 93 % double efficiency or 98 % after HR enhancement. Their system also achieved 75 %–81 % efficiency for triple disruption, indicating the potential for high-efficient gene integration in *P. pastoris*. This suggests that further optimization of the gRNA promoter and ARS elements in our system could yield even better results [33,35].

In conclusion, we identified HH-sgRNA-HDV as the most efficient sgRNA processing strategy. Based on HiEE-ReSM system, we not only achieved high efficiency of single-gene disruption, but also demonstrated the versatility of this technology both on efficient double-gene deletion and multiple genes integration at neutral sites (Table 1). In the end, we successfully applied dHgH for production of 23 mg/L/μg protein/OD FFAs and 13.3 mg/L 5-HTP using methanol as carbon source. Given the current knowledge, several potential factors to improve the positive rate of multi-locus knockout have been identified, and comprehensive optimization will likely be possible in the future. This approach facilitates the construction of a universal gRNA processing cassette with high efficiency for multiple gene disruption, thereby promoting the application of *P. pastoris* as an efficient and stable cell factory for industrial C1 biosynthesis.

4. Materials and methods

4.1. Strain, media and reagents

The yeast strain used in this study was GSY002, which improved the homologous recombination (HR) efficiency in *P. pastoris* (GS115) by knocking out the non-homologous end joining gene (*Δku70*) and overexpressing HR-related proteins (*Rad52* and *Rad59*) [14]. All plasmids and strains constructed in this study are listed in Supplementary Table 2 and Supplementary Table 3. Before transformation, first, yeast strains (GSY002) were cultivated in 2 mL of YPD medium (20 g/L glucose, 20 g/L peptone, 10 g/L yeast extract), and then the cells were cultured in 100 mL flasks with 20 mL of YPD medium to an OD_{600} of 0.6–1.0 for competent cells. Shake flask fermentation for the production of FFAs was carried out in minimal medium containing 7.5 g/L $(NH_4)_2SO_4$, 14.4 g/L KH_2PO_4, 0.5 g/L $MgSO_4•7H_2O$, 0.1 g/L histidine, 2 % methanol, trace metal, and vitamin solutions [36].

Escherichia coli strains were cultivated in Luria-Bertani (LB) media (5 g/L yeast extract, 10 g/L tryptone and 10 g/L NaCl) supplemented with 100 μg/mL hygromycin at 37 °C for plasmid construction.

Phusion™ High-Fidelity DNA Polymerase, CutSmart Buffer (10×), *Bbs*I-HF (10 U, R0535), T4 DNA ligase (40 U, M0202), and 10 mM ATP were purchased from NEB. 2× Phanta® Max Master Mix, DNA cycle purification kit, plasmid purification kit and DNA gel purification kit were purchased from Vazyme (Nanjing, China). Hygromycin was purchased from Yeasen (Shanghai, China). D-sorbitol, DL-dithiothreitol (DTT), ethylene glycol, dimethyl sulfoxide (DMSO), pentadecanoic acid, 40 % tetrabutylammonium hydroxide, methyl iodide, dichloromethane and hexane were purchased from Sigma-Aldrich.

4.2. Design and construction of the plasmid with gRNA targeting sequences

The sequences of gRNAs targeting *gut1* (UniProt ID: C4R8X4) and *aox1* (UniProt ID: P04842) were selected from published papers [6]. The gRNAs for each target gene were synthesized by Sangon Biotech (Shanghai, China). The sgRNA processing cassette consisted of a sgRNA (20 bp gRNA + scaffold) flanked with cleavable RNA sequences, including the HH-HDV ribozyme, tRNA sequences and introns. The tgt cassette contained sgRNAs flanked with tRNAs. The tgH cassette contained sgRNAs flanked with tRNA and HDV ribozyme. The HgH cassette contained sgRNAs flanked with HH and HDV ribozymes. All sequences of the 20 bp gRNAs, scaffolds and cleavable flanks are listed in Supplementary Table 4. Subsequently, all the cassettes were assembled by overlap extension (OE) PCR using multiple primers.

For the deletion of a single gene, the tgt and tgH cassettes were assembled as two modules. One module contained $tRNA^{Gly}$, while the other contained sgRNA-$tRNA^{Gly}$ or sgRNA-HDV. In the HgH cassette, the sgRNA was flanked with HH and HDV ribozymes. For the deletion of two genes, the dtgt and dtgH cassettes were assembled as three modules. In the dtgt cassette, the first module was $tRNA^{Gly}$, the second module contained sgRNA1-$tRNA^{Gly,}$ and the third module contained sgRNA2-$tRNA^{Gly}$. In the dtgH cassette, the three modules were $tRNA^{Gly}$, sgRNA1-HDV-linker-$tRNA^{Gly}$ and sgRNA-HDV. The dHgH cassette for double gene deletion was assembled as two modules consisting of HH-sgRNA1-HDV-linker and HH-sgRNA2-HDV. All modules have *Bbs*I cleavage sites on both sides, enabling them to connect with each other, and the cassettes with sgRNA can be integrated into the backbone plasmid (pBB3cH_pGAP_23_pLAT1_Cas9), a gift from Prof. Gao Xiang, which also contains the same cleavage site.

All modules were assembled by overlap extension (OE) PCR with the multiple primers listed in Supplementary Table 5, and the fragments were purified by gel purification. In the OE PCRs, 2.5 μL forward and reverse primers (10 μM), 0.5 μL inner primers (1 μM), 1 μL dNTPs (10 mM), 0.5 μL Phusion, 10 μL 5× Buffer and ddH_2O were added to compose a 50 μL mixture. The PCR procedure was set up as follows: 98 °C for 30 s; 35 cycles of 98 °C for 10 s, 60 °C for 20 s and 72 °C for 10 s; 72 °C for 2 min, and 16 °C hold.

The base vector pBB3cH_pGAP_23_pLAT1_Cas9 was digested by the restriction enzyme *Bbs*I before plasmid construction in a 50 μL reaction mixture containing 3 μg of DNA, 5 μL of 10× CutSmart Buffer and 1 μL of *Bbs*I (10 U) for at least 3 h at 37 °C. Then, Golden Gate cloning was applied for the ligation of the backbone and all fragments with sgRNAs. For a 20 μL total Golden Gate reaction, 1.6 μL of *Bbs*I, 0.1 μL of T4 ligase, 2 μL of 10× CutSmart Buffer, 2 μL of ATP (10 mM), 5 ng of *Bbs*I-digested pLAT backbone (9.3 kb), and each of the purified fragments (10 ng) were added to the reaction mixture. The Golden Gate reaction was carried out using the following PCR procedure: Step 1, 37 °C for 2 min; Step 2, 16 °C for 2.5 min; Step 3, steps 1 and 2 were repeated for 30 cycles; Step 4, 37 °C for 10 min; Step 5, 55 °C for 30 min; Step 6, 80 °C for 10 min; and Step 7, 16 °C hold.

4.3. Preparation of repairing dsDNA (donors) for gene disruption

The repairing dsDNA (donors) were assembled with a 500 bp upstream fragment and a 500 bp downstream fragment of the disrupted gene amplified from the GS115 genome using the primers listed in Supplementary Table 5. For the 50 μL PCR, 25 μL of 2× Phanta, 1 μL of each of the two oligonucleotide primers, 1 μL of the GS115 genomic template and 22 μL of ddH_2O were added to the mixture. The PCR procedure was set up at 95 °C for 10 min; 30 cycles of 95 °C for 15 s, 55 °C for 15 s and 72 °C for 15 s; 72 °C for 5 min; and 16 °C hold. After the reaction, the proteins were separated by gel purification.

4.4. Yeast transformation and calculation of positive rates

Yeast transformation was performed according to the manufacturer's protocol [37]. In detail, 4.5 mL of ice-cold BEDS solution (10 mM bicine-NaOH, pH 8.3, 3 % (v/v) ethylene glycol, 5 % (v/v) DMSO, and 1 M sorbitol) supplemented with 0.5 mL of 1 M DTT was added to the

yeast cells, which were then incubated for 5 min at 200 rpm at 30 °C. After centrifugation at 5000 rpm for 5 min, the cells were resuspended in BEDS solution. For DNA transformation, condensed electroporation (Bio-Rad Laboratories, Hercules, CA, USA) was used after adding 1 μg of Cas9 plasmid containing different sgRNA fragments and 1 μg of repair dsDNA into competent cells using the following parameters (Gene Pulser® II electroporator: cuvette gap, 2.0 mm; charging voltage, 1500 V).

To evaluate the efficiencies of the three gRNA processing cassettes, the positive rates of the transformants were calculated from three independent biological replicates (agar plates). Sixteen colonies were randomly selected from the YPD agar plates supplemented with 200 μg/mL hygromycin. After re-streaking the 16 colonies on YPD agar plates with hygromycin to remove false positives, the disruption of the targeted ORF was verified by PCR amplification using primers upstream and downstream of the ORF.

4.5. FFAs production and analysis

The sequences of gRNAs targeting *faa1* (UniProt ID: C4R1R9) and *faa2* (UniProt ID: C4R7M1) were designed from https://crispr.dbcls.jp/. The sequence of *TesA* was obtained from previous research [38]. The *faa1*, *faa2*, *fas1* (UniProt ID: C4QVT8) and *fas2* (UniProt ID: C4QY10) sequences were amplified from *P. pastoris*. *TesA* was promoted by GPM1p. *fas1* was promoted by GAPp, and *fas2* was promoted by PGIp. The sequence information is shown in Supplementary Table 5.

Fermentation of K001 and K002 was performed in shake flasks containing 15 mL of minimal media with 2 % methanol as the sole carbon source for 72 h at 200 rpm and 30 °C. Whole-cell culture FFAs were quantified as described in previous reports [20]. After 3 days of fermentation, 200 μL aliquots of cells were extracted by adding 10 μL of 40 % tetrabutylammonium hydroxide. Immediately thereafter, 200 μL of 200 mM methyl iodide in dichloromethane, containing 0.1 mg/mL pentadecanoic acid as an internal standard, was added to the mixtures. The mixtures were shaken for 30 min using a vortex mixer. After centrifugation, the dichloromethane layer was transferred into a GC vial with a glass insert and allowed to evaporate to dryness. The extracted methyl esters were then resuspended in 200 μL of dichloromethane/hexane prior to analysis by a gas chromatography-flame ionization detector (Agilent 8890 GC-FID, Agilent Technologies). The column used was an Agilent 19091J-413 HP-5 column (30 m × 320 μm × 0.25 μm, Agilent Technologies). The GC program was as follows: initial temperature of 40 °C held for 2 min; ramp to 130 °C at a rate of 30 °C per min; increase to 280 °C at a rate of 10 °C per min; and hold for 3 min. The temperatures of the inlet, mass transfer line and ion source were kept at 280 °C, 300 °C and 230 °C, respectively. The injection volume was 1 μL. The flow rate of the carrier gas (hydrogen) was set to 1.0 mL/min, and the data were acquired in full-scan mode (50–650 m z^{-1}).

The protein concentration was measured by a BCA protein assay kit (Sangon, Shanghai) as follows: a BCA working solution was prepared by mixing solution A: solution B = 50:1. The BSA standard solution was diluted to 500 μg/mL in 1× PBS (137 mM NaCl, 2.7 mM KCl, 8 mM Na_2HPO_4, $7H_2O$, and 1.5 mM KH_2PO_4, pH 7.4), and a calibration curve from 0 to 500 μg/mL with 8 points was constructed. After oscillation of 200 μL of cell broth mixed with 0.3 g of 5 mm glass beads at 2500 rpm for 10 min, the mixture was centrifuged, and the supernatant was taken as the sample. Twenty microlitres of standard or sample dilutions were added to 200 μL of BCA working solution, mixed quickly, incubated at 37 °C for 30 min, cooled, and the absorbance was measured at 562 nm. Each standard and sample were prepared with two replicates, and the final data were averaged. Finally, the FFAs titre was normalized to 1 μg of protein per OD_{600} of cell broth.

4.6. 5-HTP production and analysis

Gene *mut-tph* from previous study [29], genes *pts* (UniProt ID: P27213) and *spr* (UniProt ID: P18297) [28] were synthesized and codon optimized by GenScript (Nan Jing). The *gch1* (UniProt ID: C4QVZ7) sequence was amplified from *P. pastoris*. *mut-tph* and *spr* were promoted by GAPp, and *pts* and *gch1* was promoted by TEF1p. The sequence information is shown in Supplementary Table 5.

Fermentation of K004 was performed in shake flasks containing 15 mL of minimal media with 2 % methanol and 0.125 % glycerol as carbon sources for 72 h at 200 rpm and 30 °C. After 3 days of fermentation, 500 μL aliquots of cells were centrifugated and the supernatant was analysed by high-performance liquid chromatography (Agilent Technologies, Agilent 1260 Infinity) equipped with DAD (diode array detector). The column Agilent 5 HC-C18 (2) (150 mm × 4.6 mm) was used, and 5-HTP was separated by an isocratic elution method with 12 % methanol and 88 % phosphate buffer (10 mmol/L) at a flow rate of 1 mL/min. The data were acquired at 276 nm UV absorption.

CRediT authorship contribution statement

Kaidi Chen: Writing – original draft, Project administration, Investigation, Formal analysis. **Gulikezi Maimaitirexiati:** Writing – review & editing, Validation, Investigation. **Qiannan Zhang:** Writing – review & editing, Investigation. **Yi Li:** Writing – review & editing, Investigation. **Xiangjian Liu:** Writing – review & editing, Investigation. **Hongting Tang:** Writing – review & editing. **Xiang Gao:** Resources. **Bo Wang:** Writing – review & editing. **Tao Yu:** Writing – review & editing, Supervision. **Shuyuan Guo:** Writing – review & editing, Writing – original draft, Supervision, Conceptualization.

Funding

This work was financially supported by the National Key Research and Development Program of China (2021YFA0911000 and 2020YFA0907800), Key-Area Research and Development Program of Guangdong Province (2022B1111080005), the National Natural Science Foundation of China (NSFC 32071416), the Shenzhen Institute of Synthetic Biology Scientific Research Program (Grant No. JCHZ20200003), Shenzhen Key Laboratory for the Intelligent Microbial Manufacturing of Medicines (ZDSYS20210623091810032), and the Strategic Priority Research Program of the Chinese Academy of Sciences (XDB0480000).

Declaration of competing interest

The authors declare that they have no known competing financial interests or personal relationships that could have appeared to influence the work reported in this paper.

Acknowledgements

We thank Prof. Gao Xiang for graciously providing plasmids or strains for this project. We acknowledge the related fundings supported by China Merchants Research Institute of Advanced Technology Company Limited and China Blue Chemical Ltd.

Appendix A. Supplementary data

Supplementary data to this article can be found online at https://doi.org/10.1016/j.synbio.2025.01.005.

References

[1] Wu X, Cai P, Yao L, Zhou YJ. Genetic tools for metabolic engineering of Pichia pastoris. Engineering Microbiology 2023;3.
[2] Cai P, Duan X, Wu X, Gao L, Ye M, Zhou YJ. Recombination machinery engineering facilitates metabolic engineering of the industrial yeast Pichia pastoris. Nucleic Acids Res 2021;49:7791–805.
[3] Mali P, Yang L, Esvelt KM, Aach J, Guell M, DiCarlo JE, Norville JE, Church GM. RNA-guided human genome engineering via Cas9. Science 2013;339:823–6.
[4] Lowder LG, Zhang D, Baltes NJ, Paul 3rd JW, Tang X, Zheng X, Voytas DF, Hsieh TF, Zhang Y, Qi Y. A CRISPR/Cas9 toolbox for multiplexed plant genome editing and transcriptional regulation. Plant Physiol 2015;169:971–85.
[5] DiCarlo JE, Norville JE, Mali P, Rios X, Aach J, Church GM. Genome engineering in Saccharomyces cerevisiae using CRISPR-Cas systems. Nucleic Acids Res 2013;41:4336–43.
[6] Weninger A, Hatzl AM, Schmid C, Vogl T, Glieder A. Combinatorial optimization of CRISPR/Cas9 expression enables precision genome engineering in the methylotrophic yeast Pichia pastoris. J Biotechnol 2016;235:139–49.
[7] Geiduschek EP, Tocchini-Valentini GP. Transcription by RNA polymerase III. Annu Rev Biochem 1988;57:873–914.
[8] Dalvie NC, Leal J, Whittaker CA, Yang Y, Brady JR, Love KR, Love JC. Host-informed Expression of CRISPR guide RNA for genomic Engineering in Komagataella phaffii. ACS Synth Biol 2020;9:26–35.
[9] Gu Y, Gao J, Cao M, Dong C, Lian J, Huang L, Cai J, Xu Z. Construction of a series of episomal plasmids and their application in the development of an efficient CRISPR/Cas9 system in Pichia pastoris. World J Microbiol Biotechnol 2019;35:79.
[10] Knapp D, Michaels YS, Jamilly M, Ferry QRV, Barbosa H, Milne TA, Fulga TA. Decoupling tRNA promoter and processing activities enables specific Pol-II Cas9 guide RNA expression. Nat Commun 2019;10:1490.
[11] Shechner DM, Hacisuleyman E, Younger ST, Rinn JL. Multiplexable, locus-specific targeting of long RNAs with CRISPR-Display. Nat Methods 2015;12:664–70.
[12] Gao Y, Zhao Y. Self-processing of ribozyme-flanked RNAs into guide RNAs in vitro and in vivo for CRISPR-mediated genome editing. J Integr Plant Biol 2014;56:343–9.
[13] Zhang K, Duan X, Cai P, Gao L, Wu X, Yao L, Zhou YJ. Fusing an exonuclease with Cas9 enhances homologous recombination in Pichia pastoris. Microb Cell Fact 2022;21:182.
[14] Wang X, Li Y, Jin Z, Liu X, Gao X, Guo S, Yu T. A novel CRISPR/Cas9 system with high genomic editing efficiency and recyclable auxotrophic selective marker for multiple-step metabolic rewriting in Pichia pastoris. Synth Syst Biotechnol 2023;8:445–51.
[15] Xie K, Minkenberg B, Yang Y. Boosting CRISPR/Cas9 multiplex editing capability with the endogenous tRNA-processing system. Proc Natl Acad Sci U S A 2015;112:3570–5.
[16] Zhang Y, Wang J, Wang Z, Zhang Y, Shi S, Nielsen J, Liu Z. A gRNA-tRNA array for CRISPR-Cas9 based rapid multiplexed genome editing in Saccharomyces cerevisiae. Nat Commun 2019;10:1053.
[17] Qi W, Zhu T, Tian Z, Li C, Zhang W, Song R. High-efficiency CRISPR/Cas9 multiplex gene editing using the glycine tRNA-processing system-based strategy in maize. BMC Biotechnol 2016;16:58.
[18] Shiraki T, Kawakami K. A tRNA-based multiplex sgRNA expression system in zebrafish and its application to generation of transgenic albino fish. Sci Rep 2018;8:13366.
[19] Lennen RM, Pfleger BF. Engineering Escherichia coli to synthesize free fatty acids. Trends Biotechnol 2012;30:659–67.
[20] Zhou YJ, Buijs NA, Zhu Z, Qin J, Siewers V, Nielsen J. Production of fatty acid-derived oleochemicals and biofuels by synthetic yeast cell factories. Nat Commun 2016;7:11709.
[21] Gibson DG, Glass JI, Lartigue C, Noskov VN, Chuang RY, Algire MA, Benders GA, Montague MG, Ma L, Moodie MM, et al. Creation of a bacterial cell controlled by a chemically synthesized genome. Science 2010;329:52–6.
[22] Hutchison CA, Chuang RY, Noskov VN, Assad-Garcia N, Deerinck TJ, Ellisman MH, Gill J, Kannan K, Karas BJ, Ma LJS. Design and synthesis of a minimal bacterial genome, vol. 351; 2016aad6253.
[23] Maffei ME. 5-Hydroxytryptophan (5-HTP): natural occurrence, analysis, biosynthesis, Biotechnology, physiology and toxicology. Int J Mol Sci 2020;22.
[24] Fitzpatrick PF. Tetrahydropterin-dependent amino acid hydroxylases. Annu Rev Biochem 1999;68:355–81.
[25] Rolfes RJ. Regulation of purine nucleotide biosynthesis: in yeast and beyond. Biochem Soc Trans 2006;34:786–90.
[26] Wolff DW, Bianchi-Smiraglia A, Nikiforov MA. Compartmentalization and regulation of GTP in control of cellular phenotypes. Trends Mol Med 2022;28:758–69.
[27] Thony B, Auerbach G, Blau N. Tetrahydrobiopterin biosynthesis, regeneration and functions. Biochem J 2000;347(Pt 1):1–16.
[28] Germann SM, Baallal Jacobsen SA, Schneider K, Harrison SJ, Jensen NB, Chen X, Stahlhut SG, Borodina I, Luo H, Zhu J, et al. Glucose-based microbial production of the hormone melatonin in yeast Saccharomyces cerevisiae. Biotechnol J 2016;11:717–24.
[29] Zhang Z, Yu Z, Wang J, Yu Y, Li L, Sun P, Fan X, Xu Q. Metabolic engineering of Escherichia coli for efficient production of L-5-hydroxytryptophan from glucose. Microb Cell Fact 2022;21:198.
[30] Saint-Marc C, Pinson B, Coulpier F, Jourdren L, Lisova O, Daignan-Fornier B. Phenotypic consequences of purine nucleotide imbalance in Saccharomyces cerevisiae. Genetics 2009;183:529–38. 521si-527si.
[31] Guo Y, Liao Y, Wang J, Ma C, Qin J, Feng J, Li Y, Wang X, Chen K. Methylotrophy of Pichia pastoris: current advances, applications, and future perspectives for methanol-based biomanufacturing. ACS Sustainable Chem Eng 2022;10:1741–52.
[32] Liao X, Li L, Jameel A, Xing XH, Zhang C. A versatile toolbox for CRISPR-based genome engineering in Pichia pastoris. Appl Microbiol Biotechnol 2021;105:9211–8.
[33] Gao J, Xu J, Zuo Y, Ye C, Jiang L, Feng L, Huang L, Xu Z, Lian J. Synthetic Biology Toolkit for marker-less Integration of multigene Pathways into Pichia pastoris via CRISPR/Cas9. ACS Synth Biol 2022;11:623–33.
[34] Liu Q, Shi X, Song L, Liu H, Zhou X, Wang Q, Zhang Y, Cai M. CRISPR-Cas9-mediated genomic multiloci integration in Pichia pastoris. Microb Cell Fact 2019;18:144.
[35] Gao J, Ye C, Cheng J, Jiang L, Yuan X, Lian J. Enhancing homologous recombination Efficiency in Pichia pastoris for multiplex genome integration using short homology arms. ACS Synth Biol 2022;11:547–53.
[36] Yu T, Zhou YJ, Huang M, Liu Q, Pereira R, David F, Nielsen J. Reprogramming yeast metabolism from alcoholic fermentation to lipogenesis. Cell 2018;174:1549–58. e1514.
[37] Lin-Cereghino J, Wong WW, Xiong S, Giang W, Luong LT, Vu J, Johnson SD, Lin-Cereghino GP. Condensed protocol for competent cell preparation and transformation of the methylotrophic yeast Pichia pastoris. Biotechniques 2005;38(44):46. 48.
[38] Hou R, Gao L, Liu J, Liang Z, Zhou YJ, Zhang L, Zhang Y. Comparative proteomics analysis of Pichia pastoris cultivating in glucose and methanol. Synth Syst Biotechnol 2022;7:862–8.